Observation of a Precursor during the Crystallization of Amorphous $NiZr_2$

M. Sutton, Y. S. Yang, and J. Mainville
Department of Physics, McGill University, 3600 University Street, Montreal, Quebec, Canada H3A 2T8

J. L. Jordan-Sweet, K. F. Ludwig, Jr., and G. B. Stephenson
IBM Research Division, Thomas J. Watson Research Center, Yorktown Heights, New York 10598
(Received 15 June 1988)

In situ studies of the isothermal crystallization of an amorphous alloy ($NiZr_2$) have been performed using time-resolved x-ray diffraction, with a time resolution as short as 3 ms. In the temperature range studied (628–680 K), a transient structural precursor is present during the crystallization. The maximum volume fraction reached by this precursor during crystallization increases with the rate of crystallization.

PACS numbers: 64.70.Kb, 61.10.Gs, 64.60.My, 64.60.Qb

Many materials can be taken out of equilibrium by rapidly quenching them through a phase transformation. The resulting evolution towards equilibrium provides interesting examples of nonequilibrium phenomena. The ability to measure x-ray diffraction patterns in real time with millisecond resolution allows for more comprehensive studies of phase-transition kinetics.

A classic example of a first-order phase transition is the crystallization of an amorphous material, the kinetics of which is governed by nucleation and growth. The crystallization rate has a maximum at a temperature somewhat below the freezing point. This maximum is determined by a tradeoff between the decreasing free energy of the transformation and the increasing atomic mobility as the sample temperature is increased.[1] However, structural studies of crystallization in amorphous metals have only been done at temperatures well below the maximum rate. In this Letter we present time-resolved x-ray diffraction measurements on the crystallization of amorphous $NiZr_2$, a model metallic glass. The x-ray scattering geometry chosen allows us to monitor crystallization on an unprecedented millisecond time scale. Using this technique, we have observed an unexpected transient structure which occurs under conditions of extremely rapid crystallization.

Ni_xZr_{1-x} can be made amorphous over a large composition range ($x=0.2$ to 0.85) by melt spinning.[2] The composition chosen for this study ($x=\frac{1}{3}$) corresponds to the congruently melting compound $NiZr_2$ on the equilibrium phase diagram, which has a body-centered tetragonal crystal structure[3] $D_{4h}^{18}(I4/mcm)$. Amorphous $NiZr_2$ is therefore expected to crystallize, with only local structural changes and no long-range compositional segregation, into single-phase crystalline $NiZr_2$. Calorimetry studies of the crystallization[2] show a single well-defined exothermic peak at this composition. This polymorphic crystallization should provide a simple, model system in which to study the kinetics of crystallization.

A detailed description of our experimental setup has been previously published.[4] During a typical crystallization run, a ribbon of $NiZr_2$ is resistively self-heated from room temperature to a constant final temperature. Simultaneously, the x-ray diffraction profile, sample resistance, and sample temperature are recorded as functions of time. Samples are ribbons of width 1.5 mm, thickness 15 μm, and length 50 mm. The sample temperature is measured by an infrared pyrometer, which is calibrated by comparing our low-temperature crystallization rates to the literature values. The time origin ($t=0$) is defined to be the time at which the sample temperature reaches 99% of its final value.

Experiments were performed at the National Synchrotron Light Source with the IBM-MIT beam line X20C. The essential features of this beam line[5] are a 1:1 focusing mirror which gives a focal spot of 1 mm by 1 mm at the sample position, and a wide bandpass monochromator incorporating artificial multilayer structures of tungsten and silicon having a period of 23 Å. At the energy used (6.0 keV), the monochromator has an energy bandpass of 0.55%, half width at half maximum. With a current of 100 mA in the synchrotron ring, the beam line provides an intensity in the incident beam of 10^{13} counts/s. Diffraction profiles are measured in reflection by a position-sensitive detector consisting of a photodiode array with 1024 elements spanning 25 mm. The detector is placed 95 mm from the sample and centered at a scattering angle of 50°. For this experiment the diodes are electronically grouped by 16 to form an array of 64 pixels. The absorption length of $NiZr_2$ at 6 keV is 6 μm so half the scattering intensity comes from the top 1 μm of the sample. The count rate from our samples is in excess of 100000 counts/s in the pixel at the maximum of the crystal peaks and about half that at the amorphous peak. As shown in Ref. 4, a diffraction pattern could be acquired as fast as every 3 ms. For lower temperatures, where the slower kinetics allowed for time resolutions of 1 s or more, volume crystal frac-

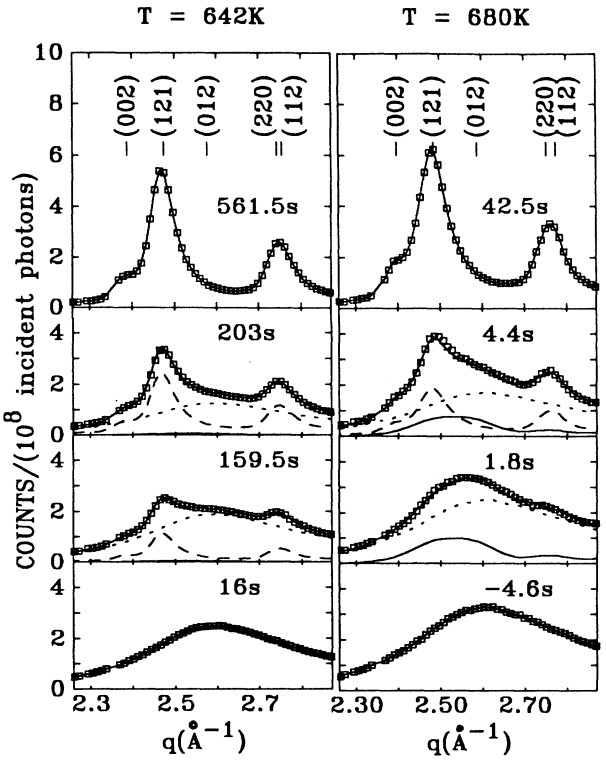

FIG. 1. Diffraction patterns for a representative time sequence at two annealing temperatures. Symbols represent measured x-ray scattering and the solid lines through them are the results of the fit by Eq. (1). The individual components are also plotted for each pattern. The amorphous contribution is dotted, the crystalline contribution is dashed, and the precursor contribution is solid. The times selected are based on the time it takes to reach $X=0\%$, 25%, 50%, and 100% total volume crystal fraction. The time per diffraction pattern is 1.5 s for $T=642$ K and 0.2 s for $T=680$ K. The negative time corresponds to a time during the heating.

tions as small as 0.1% could be measured.

Figure 1 shows the scattering intensity as a function of wave number (q) at various times during the crystallization. Data from two runs at different anneal temperatures are plotted as points. One can see the diffraction peaks of the crystalline phase growing at the expense of the broader peak of the amorphous phase. The widths of the diffraction peaks of the crystal phase do not change with time. This indicates that the average crystal size is always larger than our resolution limit (≈ 100 Å) for observable volume fractions. Even without detailed analysis, a difference between the scattering profiles at the two temperatures can be seen. The data at $T=642$ K are adequately described by a linear superposition of the initial amorphous and the final crystalline scattering pattern, but at 680 K the data cannot be so simply described. It is found that the scattering data for all temperatures studied can be explained by the inclusion of a transient broad scattering pattern. The appearance of this extra scattering is a precursor to the onset of crystallization.

Lines through the data in Fig. 1 are fits to the diffraction patterns with the assumption of a linear decomposition of each scattering pattern into three separate parts: an amorphous pattern $I_a(q)$; a crystalline pattern $I_c(q)$; and a transient, precursor pattern $I_p(q)$. Explicitly, the scattering intensity used is

$$I(q,t)=[1-X(t)]I_a(q) + X(t)\{[1-f(t)]I_c(q)+f(t)I_p(q)\}, \quad (1)$$

where $X(t)$ is the total volume fraction transformed and $f(t)$ is the precursor fraction of the transformed volume. The amorphous and crystalline diffraction patterns, I_a and I_c, are simply the measured patterns shown for the initial and final times, respectively. Before we discuss the functional form used for the precursor pattern, several other observations will be made about the data. The times shown correspond to $X=0\%$, 25%, 50%, and 100%. The contribution of the transient precursor is most pronounced during crystallization at higher temperatures, and thus faster rates. Even though the precursor contribution is small at the lower temperature, it must be included in order for the amorphous volume fraction decrease to be matched by a corresponding increase in the transformed volume fraction.

Figure 2 shows the measured sample temperature, resistance, and total and precursor volume fractions plotted as functions of time for three anneal temperatures. It can be seen that the initial loss of amorphous scattering is taken up solely by an increase in the precursor scattering. Another striking feature shown in this figure is the initial increase in resistivity seen for the high temperatures prior to the expected decrease due to crystallization. The increase and decrease in resistivity correlate with the increase and decrease in the amount of precursor scattering.

The volume fraction $X(t)$ as a function of time may be represented by[1]

$$-\ln(1-X)=\gamma^3\int_0^t I(t')(t-t')^3\,dt', \quad (2)$$

where γ is a linear growth rate. $I(t)$ is the time-dependent nucleation rate given by an approximate theory of transient nucleation[1] as

$$I(t)=I_0\left[1+2\sum_{m=1}^{\infty}(-1)^m\exp(-m^2t/\tau)\right], \quad (3)$$

where τ is called the incubation or induction time and I_0 is the steady-state nucleation rate. Figure 3 shows how well such a simple model works for $T=642$ K. The deviation of the fit for volume fractions above $X=40\%$ is an artifact of finite size.[6] These fits cannot be considered a stringent test of the transient nucleation theory since steady-state nucleation is reached at a time equal to or

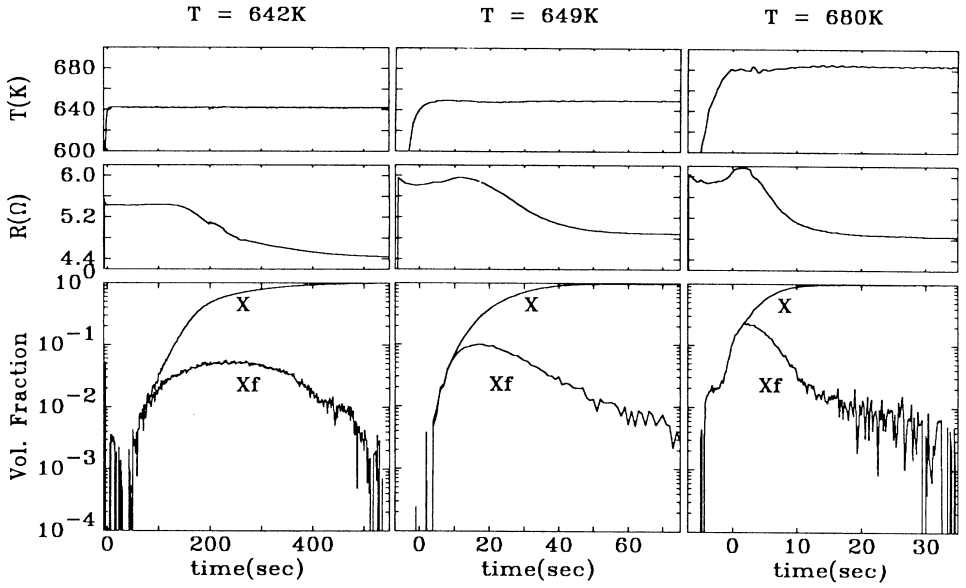

FIG. 2. The time dependence of resistance (R), temperature (T), total volume crystal fraction (X), and precursor volume crystal fraction (Xf) for three annealing temperatures. Note that isothermal conditions are obtained with little or no overshoot in temperature, although at the highest temperatures crystallization starts before a constant temperature is reached.

less than the time at which a measurable volume fraction is reached. For the three low temperatures 628, 635, and 642 K, the temperature dependences of τ and $\gamma^3 I_0$ are consistent with an Arrhenius behavior. The activation energy of 3 eV is in agreement with calorimetric data.[2] The temperature dependence is reasonable since the kinetics is expected to be dominated by the temperature dependence of the mobility for this temperature range. For the higher two temperatures in Fig. 2, heating times are comparable to crystallization times. These curves are consistent with the low-temperature data, after a reasonable offset is made to $t=0$, if the contribution of the precursor scattering is included.

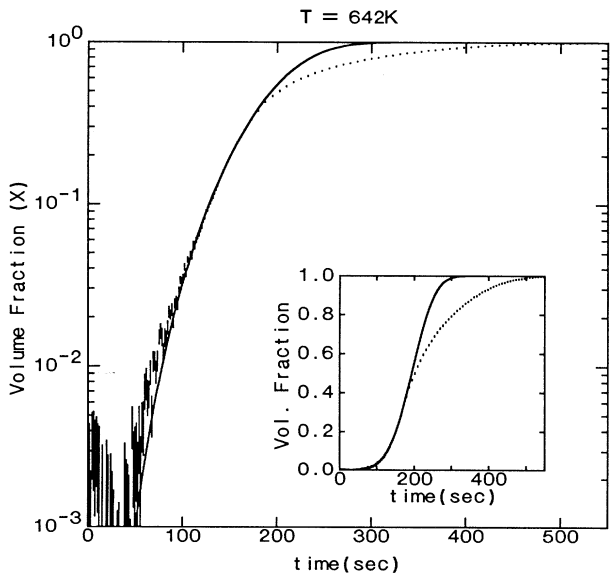

FIG. 3. The time dependence of the volume crystal fraction for $T=642$ K. The solid curve is a fit by Eq. (2) as discussed in the text, with $\tau=13.1$ s and $\gamma^3 I_0=3.9\times10^{-7}$ s^{-4}. Inset: the volume fraction on a linear scale. For times longer than 150 s, only every fifth data point is shown.

The evidence shows that the extra scattering must be associated with the nucleation process. That the precursor scattering increases with temperature is consistent with a higher nucleation rate and the associated increase in number of particles of a given volume fraction, X. A large number of small crystallites could also explain the increase in resistance seen at the higher temperatures. The Arrhenius behavior of the total volume fraction $X(t)$ implies that the precursor is an intrinsic part of the crystallization process. At high nucleation rates it would be expected that some effect would be observed in the scattering due to the interfacial region between the glass and crystalline material. That the transient scattering is seen with little or no crystalline scattering suggests a modified model in which nucleation occurs into a poorly ordered crystal structure. The disordered structure then converts into the equilibrium crystal structure. As the particles grow, the disorder is maintained at the interface between the crystalline and the amorphous phases. For the higher-temperature runs, the poorly ordered region must occupy a significant fraction of a particle's volume in order to account for the large volume fraction observed. The growth of the particles would then occur by the transition of material from the amorphous to the precursor structure and the observed Arrhenius behavior

would be a reflection of this transition. Obviously more work is needed to understand these rapid crystallizations.

From Fig. 1, it can be seen that the precursor scattering is a broad peak intermediate between the (121) crystalline Bragg peak and the amorphous peak. To attribute a structure unambiguously to this scattering pattern is not possible. A model in which the precursor scattering arises from an asymmetric distortion of the (121) Bragg peak seems improbable as it is hard to imagine a shift as large as 0.1 $Å^{-1}$. The functional form, $I_p(q)$, used to fit the precursor scattering in this Letter is based on the calculated $NiZr_2$ crystal diffraction pattern which is modified by our including the normally forbidden (012) Bragg peak and increasing the width of the individual peaks. The precursor fraction $f(t)$ was normalized to unity by the fitting of a single diffraction pattern at a time near its maximum. The resulting integrated intensity for I_p was found to be comparable to the integrated intensity for the fully crystallized sample. Further evidence for this type of modification is the observation of a transient peak at the forbidden (221) position. The existence of these peaks would follow from a structure in which the atoms at the tetragonal body centers sometimes differ from those at the origins, perhaps because of an incompletely formed crystal structure or partial exchange of Ni and Zr. The fact that the time scales for $X(t)$ and $f(t)$ are similar over the temperature range studied seems to indicate that this structure is a nonequilibrium structure which relaxes to the equilibrium $NiZr_2$ structure and probably is not a separate phase. Finally, it should be noted that transmission electron microscope studies[7] indicate an unusual morphology for the crystallites in partially crystallized $NiZr_2$.

If precursor structures turn out to be a general feature of nucleation and growth at high rates, a reevaluation of classical theories would be required since they assume the coexistence of the initial and final structures. Whether or not transient structures turn out to be common in nucleation and growth, the ability to measure structural information with millisecond time resolution has allowed us to experimentally address issues and study mechanisms at a level of detail not previously possible. These experimental results demonstrate the potential that now exists for new studies into nucleation and growth phenomena in liquids, thin films, and amorphous solids.

We would like to thank John Strom-Olsen and Zaven Altounian for teaching us how to make the samples and for sharing their expertise and we would like to acknowledge many useful discussions with Martin Grant and Dik Harris. Part of this work has been supported by the Natural Sciences and Engineering Research Council of Canada. The MIT part of the IBM-MIT consortium is supported by the National Science Foundation, Materials Research Laboratory Program under Grant No. DMR84/18718. The National Synchrotron Light Source is supported by the U.S. Department of Energy, Division of Materials Sciences and Division of Chemical Sciences (DOE Contract No. DE-AC02-76CH00016).

[1]J. W. Christian, *The Theory of Transformations in Metals and Alloys* (Pergamon, New York, 1975), 2nd ed. Pt. 1.

[2]Z. Altounian, Guo-Hua Tu, and J. O. Strom-Olsen, J. Appl. Phys. **54**, 3111–3116 (1983).

[3]M. E. Kirkpatrick, D. M. Bailey, and J. F. Smith, Acta Crystallogr. **15**, 252 (1962).

[4]M. Sutton, Y. S. Yang, J. Mainville, J. O. Strom-Olsen, Z. Altounian, G. B. Stephenson, and K. F. Ludwig, Jr., in *Proceedings of the Sixth International Conference on Rapidly Quenched Metals (RQ6),* edited by R. W. Cochrane and J. O. Strom-Olsen [Mater. Sci. Eng. **97**, 307–311 (1988)].

[5]G. B. Stephenson, Nucl. Instrum. Methods Phys. Res. Sect. A **266**, 447 (1988).

[6]As the size of the crystallites becomes comparable to the observation depth, the increase in X due to growth away from the surface cannot be seen. This results in a slowing of the observed volume fraction increase, which is not taken into account by the theory.

[7]J. L. Walter, Z. Altounian, and J. O. Strom-Olsen, J. Non-Cryst. Solids **61/62**, 463 (1984); Y. C. Feng, K. H. Kuo, Z. K. Hei, and Y. K. Wu, Philos. Mag. A **56**, 757 (1987).